

Facile Preparation of PLGA Microspheres With Diverse Internal Structures by Modified Double-Emulsion Method for Controlled Release

Fengxuan Han, Fang Zhou, Xiaoling Yang, Jin Zhao, Yunhui Zhao, Xiaoyan Yuan

School of Materials Science and Engineering, and Tianjin Key Laboratory of Composite and Functional Materials, Tianjin University, Tianjin 300072, China

Poly(L-lactide-co-glycolide) (PLGA) microspheres with diverse internal structures and different release behaviors were prepared via a modified double-emulsion method by introduction of heparin or carboxymethyl chitosan in the inner aqueous phase and calcium chloride in the outer aqueous phase, respectively. The main factors affecting the microsphere morphology were systematically studied, including compositions in the inner aqueous phase, the oily phase, and the outer aqueous phase. The transmission electron microscope images demonstrated that the microspheres are featured with single core, hollow, and multicore structures when their sizes were less than 200 nm, in the range of 200–700 nm, and greater than 700 nm, respectively. In comparison with hollow PLGA microspheres, the PLGA microspheres with heparin and carboxymethyl chitosan in the inner aqueous phase also showed multicore and single core structures, respectively, and exhibited higher loading efficiencies and slower release rates by using bovine serum albumin as a model for bioactive substances. It was concluded that this study provided a facile method to prepare microspheres with single core, multicore, or hollow feature, and the tunability of the different internal structures and related release profiles enables these systems cater to specific requirements for potential applications in controlled biomolecule delivery for tissue regeneration. POLYM. ENG. SCI., 55:896–906, 2015. © 2014 Society of Plastics Engineers

INTRODUCTION

In recent years, entrapments of proteins and genes in microspheres or microcapsules prepared from the biodegradable and biocompatible polymers were widely investigated. Among these polymers, polylactide (PLA), and poly(L-lactide-co-glycolide) (PLGA) have attracted growing attention [1, 2]. Now, the PLA or PLGA microspheres with good biocompatibility and biodegradation have been used for incorporating bone morphogenetic protein and leuporelin acetate and applications or interactions with the eye, central nervous system, and lymphoid tissue and their relevance to vaccine development [3]. Especially, hollow microspheres, core/shell or double-walled microspheres having a biomolecule-encapsulation core and biomolecule-free shell would be suitable for controlled delivery carriers to attain well-

controlled release rates [4, 5]. The folate-decorated PEG-PLGA nanoparticles with silica shells were prepared and had high potential to be used for targeted and controlled drug delivery [6]. The dextran/PLGA-PLA core/shell microspheres were prepared to load interleukin-2 (rIL-2) and exhibited sustained release behavior for rIL-2, and the microspheres showed better local efficacy at the tumor site in the mice [7].

A number of microencapsulation techniques have been developed to entrap proteins into microcapsules or microspheres, including double-emulsion, organic phase separation and spray drying [8, 9]. The emulsion process was common to prepare microspheres, and most of the microspheres prepared from the emulsion method had a multi-core internal structure. Meanwhile, these emulsions could be used to create solid particles by adding various functional materials into the disperse phase [10, 11]. Double or multiple emulsions were also applied to produce particles with hollow, core-shell or double-walled structure [12]. Albuquerque et al. fabricated double-walled poly(L-lactide) (PLLA)-PLGA microspheres containing meloxicam by using the technique of oil-in-water-in-water emulsion and solvent evaporation. The phase separation of the two polymers during the solvent evaporation resulted in the double-walled structure, and the composition of shell and core could be modulated by controlling the PLLA/PLGA mass ratio [13]. Hollow microspheres of a methacrylic acid copolymer could also be prepared by the emulsion solvent diffusion method [14]. An emulsifier, for example poly(vinyl alcohol) (PVA), was commonly used to stabilize the double-emulsion during the process. However, a certain amount of residual PVA on the surface was proved to affect the particle properties [15]. An improvement for double-emulsion method was achieved by replacing PVA with calcium chloride (CaCl₂), and the outer aqueous phase of the CaCl₂ solution in this experiment could accelerate microsphere solidification [16].

Improved methods including emulsion polymerization and microfluidic technology were also brought about to prepare solid core, hollow, core/shell or double-walled polymer particles [17–19]. For example, a one-step photo-initiated miniemulsion polymerization was applied to prepare core-shell structure epoxy-functionalized magnetic polymer microspheres [17]. A soap-free emulsion polymerization was also used to prepare polystyrene/poly(o-toluidine) (PS/POT) microspheres, and the resultant spheres show double-shelled hollow structure with PS as internal walls and POT as exterior shells, and the benefits of this method were neither organic solvents nor high-temperature calcinations for removing PS template [18]. Microfluidic technology was a simple method to prepare uniform solid core, core-shell or double-walled microspheres [19], but the obtained relatively big sized microspheres and the special microfluidic devices required usually limited their applications.

Correspondence to: X. Yuan; e-mail: yuanxy@tju.edu.cn

Contract grant sponsor: Natural Science Foundation of China; contract grant number: 51073117.

Contract grant sponsor: Scientific Research Foundation of Graduate School of Tianjin University.

DOI 10.1002/pen.23957

Published online in Wiley Online Library (wileyonlinelibrary.com).

© 2014 Society of Plastics Engineers

The morphology and composition of the microspheres had great effects on the release behaviors of biomolecules. By adjusting the preparation conditions, the inner microbubble structure could be obtained [20]. Zheng et al. [21] prepared composite microspheres of alginate-chitosan-PLGA that showed higher loading efficiency than those in the conventional PLGA microspheres because the alginate-chitosan core created protein-friendly micro-environment which could avoid protein denaturation.

It was firstly found in this study that the internal structure of PLGA microspheres were affected by changing the preparation conditions of a modified double-emulsion technology. This phenomenon was interesting, and it was necessary to systematically investigate the influencing factors on the morphology and structure of the resulting PLGA microspheres including the internal and outer aqueous phase composition, oily phase composition, and the volume ratio of inner aqueous phase to oily phase. To evaluate the loading and release behavior of the PLGA microspheres for bioactive substances, bovine serum albumin (BSA) was selected as the model protein and loaded into three typical kinds of microspheres by introduction of heparin or carboxymethyl chitosan with different internal structures and compositions to study their controlled release behaviors *in vitro*. Applications of the PLGA microspheres in encapsulating growth factors will be studied in the further studies.

EXPERIMENTAL METHOD

Materials

Poly(L-lactide-co-glycolide) (PLGA, LA/GA=50/50, $\overline{M}_w=1.9 \times 10^4$, $\overline{M}_n=1.4 \times 10^4$) was synthesized by ring-opening polymerization using ethylene glycol or poly(ethylene glycol) as the initiator in the presence of stannous octoate [22]. Carboxymethyl chitosan ($\overline{M}_w=9000$) was provided by Shan Dong Ao Kang Biochemical Co., China. Heparin sodium was purchased from Tianjin Lianxing Biotechnology Co., China. BSA and Pluronic F127 were purchased from Sigma-Aldrich Co., US. Calcium chloride and sodium chloride were provided by Shanghai Sangon Biological Engineering Co., China. Chloroform (CHCl_3), dichloromethane (CH_2Cl_2), and *N,N*-dimethyl formamide (DMF) were all supplied by Tianjin Kermel Chemical Reagent Co., China.

Preparation of PLGA Microspheres by the Modified Double-Emulsion Method

The PLGA microspheres were prepared by the modified water/oil/water double-emulsion method as shown in Fig. 1. PLGA and a certain amount of F127 were dissolved in CH_2Cl_2 to form the oily phase (O). Meanwhile, BSA or a certain amount of carboxymethyl chitosan or heparin sodium was dissolved in PBS (pH 7.4, 0.1 M) in a certain concentration to obtain inner aqueous phase (W1). The W1 was dispersed into O phase by sonication over an ice bath (56W, 60s). A CaCl_2 solution was used as the outer aqueous phase (W2) according to the reference [16]. The resulting primary emulsion (W1/O) was dropped into deionized water containing CaCl_2 at 2/5 volume ratio under sonication over an ice bath (112 W, 300 s). The obtained double-emulsion was placed under magnetic stirring for 4 h to evaporate organic solvent at room temperature, and the hardened PLGA microspheres were dialyzed for 3 h in deionized water. After freeze-drying, the microspheres were

stored at -20°C . Different preparation conditions were used to check the influence of the inversion on microsphere morphology and internal structure, and the experimental parameters were summarized in Table 1.

Characterizations

The prepared microspheres were viewed under an optical microscope (OM, BX51, Japan), a scanning electron microscope (SEM, Philips XL-30) and a transmission electron microscope (TEM, JEOL JEM-100CX II), respectively. The average microsphere size was estimated from SEM micrographs in the original magnification of 10,000 using Adobe Photoshop software. The internal structure of microsphere was examined by the TEM micrographs. For the TEM observation, the obtained microspheres were dispersed in ethanol and then dropped onto a carbon-coated copper mesh directly.

In Vitro Release

BSA was chosen as a model for bioactive substance and loaded in the aqueous phase W1, and the obtained PLGA microspheres were recorded as sample MS. Heparin was negative and usually used for protecting bioactive and controlled release of growth factors [23], whereas carboxymethyl chitosan was positive which may be used to control delivery of proteins and DNA with negative charge. To determine the effect of the W1 composition and internal structure on the BSA release behaviors, heparin sodium or carboxymethyl chitosan were introduced into W1, and the prepared microspheres were designated as MS-H and MS-C, respectively. The detailed preparation conditions for MS, MS-H and MS-C were listed in Table 2. The release behaviors of MS, MS-H and MS-C samples were determined by adding 10 mg microspheres into each centrifuge tube filled with 2.0 mL of PBS (pH 7.4, 0.1 M) containing 0.1% (*wt/v*) sodium dodecyl sulphate. Then the tubes were moved in a shaking water bath at 37°C . At predetermined time intervals (30 min, 12 h, 1 d, 2 d, 4 d, 7 d, 10 d, 14 d, 21 d, 28 d, 42 d, 56 d and 70 d), 0.6 mL of the initially buffer was removed for analysis, and 0.6 mL fresh PBS was added. The amount of BSA in the release medium was detected using an ELISA reader (Biorad 450) at wavelength of 562 nm with micro BCA protein assay reagent kit (Pierce, Thermo scientific, USA). Cumulative BSA release profiles were calculated, and the total amount of BSA encapsulated in microspheres was composed of the released portion during the incubation and the portion in residual microspheres. The residual BSA in the microspheres was determined using method in the previous report [24]. In short, the microspheres were degraded in 2 mL NaOH solution (1 M) with sodium dodecyl sulphate (0.1%, *wt/v*) and then the solution was adjusted to about pH 7.4. The BSA concentration was estimated using a micro BCA assays method as described above. Three repetitions were performed for each sample, and the results are presented as means \pm SD.

RESULTS AND DISCUSSION

The release behaviors were affected by the microspheres morphology and composition. Several studies have examined effects of parameters such as the volume of inner aqueous phase, the polymer molecular weight, the outer aqueous

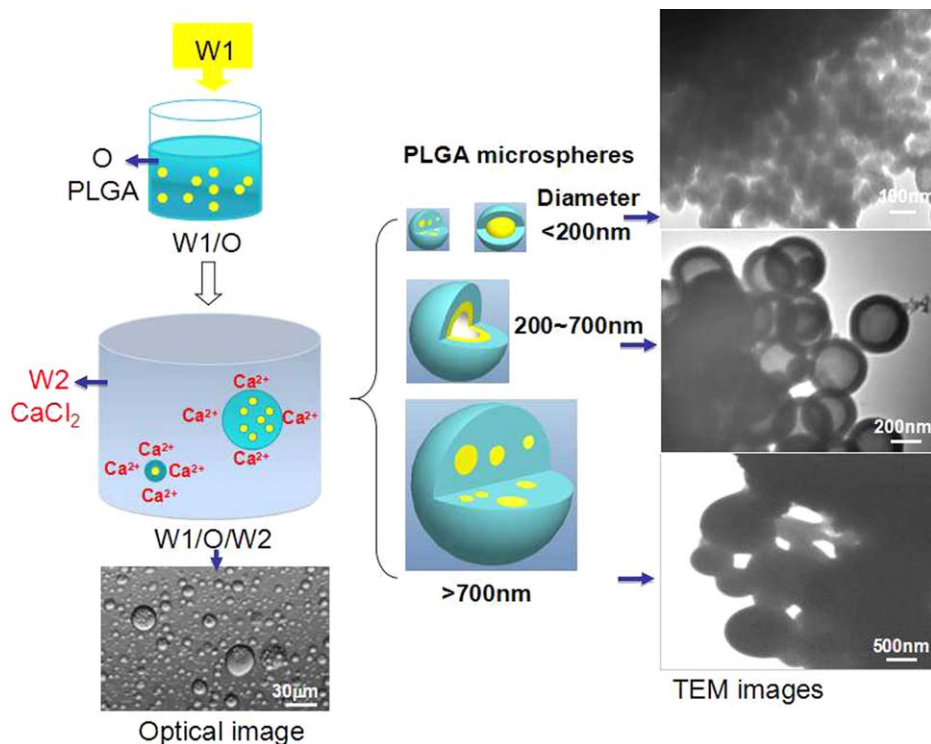


FIG. 1. Schematic diagram of the modified double-emulsion method for PLGA microspheres preparation, and microspheres with wide size distribution showed single core, multicore and hollow internal structures under a given condition (Table 1, A1) depending on the emulsion instability, solvent evaporation and polymer solidification. The optical image shows the double-emulsion containing liquid droplets with different sizes. The TEM images show PLGA microspheres with various diameters and different internal structures, solid or hollow. [Color figure can be viewed in the online issue, which is available at wileyonlinelibrary.com.]

composition, and organic solvent on the PLGA particles size [25, 26]. This experiment investigated the influence of preparation parameters on the shape and internal structure of the micro-

spheres and to refine optimal parameters for fabricating microspheres with the most uniform morphology and internal structure. The discussions were focused on the factors, i.e., W1

TABLE 1. Conditions for the preparation of PLGA microspheres.

| No. ^a | W1/O | | | | | | W1/O/W2 | | |
|------------------|-------------|----------------------------------|----|-------------------------------------|---------------------------------|-------------------|------------|-----|---------------------------|
| | W1 | | O | Organic solvent | | | W1:O (v/v) | W2 | |
| | BSA (mg/mL) | CS ($\bar{M}_w=9,000$) (mg/mL) | | PLGA ($\bar{M}_n=19,000$) (mg/mL) | CH ₂ Cl ₂ | CHCl ₃ | | DMF | CaCl ₂ (mg/mL) |
| A1 | – | – | 10 | √ | – | – | 1:3 | 2 | – |
| A2 | – | – | 10 | √ | – | – | 1:5 | 2 | – |
| A3 | – | – | 10 | √ | – | – | 1:10 | 2 | – |
| B1 | – | – | 10 | √ | – | – | 1:3 | 2 | – |
| B2 | 10 | – | 10 | √ | – | – | 1:3 | 2 | – |
| B3 | – | 50 | 10 | √ | – | – | 1:3 | 2 | – |
| B4 | 10 | 50 | 10 | √ | – | – | 1:3 | 2 | – |
| C1 | 10 | – | 10 | √ | – | – | 1:3 | 2 | – |
| C2 | 10 | – | 10 | – | √ | – | 1:3 | 2 | – |
| C3 | 10 | – | 10 | – | – | √ | 1:3 | 2 | – |
| D1 | 10 | – | 10 | √ | – | – | 1:3 | – | – |
| D2 | 10 | – | 10 | √ | – | – | 1:3 | – | 2 |
| D3 | 10 | – | 10 | √ | – | – | 1:3 | 0.5 | – |
| D4 | 10 | – | 10 | √ | – | – | 1:3 | 2 | – |

^aGroup A: different volume ratios of W1/O in the primary emulsion; Group B: different W1 solutions; Group C: different organic solvents; Group D: different W2 solutions.

TABLE 2. Compositions for the preparation of MS, MS-H, and MS-C microspheres.

| Sample | W1 | | | Other conditions | BSA encapsulation efficiency (%) |
|--------|-------------|---------------------------------------|-----------------|--|----------------------------------|
| | BSA (mg/mL) | CS ($\overline{M}_w=9,000$) (mg/mL) | Heparin (mg/mL) | | |
| MS | 10 | – | – | 10 mg/mL PLGA | 28.7 ± 0.4 |
| MS-H | 10 | – | 50 | ($\overline{M}_n=19,000$) in CH ₂ Cl ₂ ; | 39.4 ± 0.9 |
| MS-C | 10 | 50 | – | W1/O=1/3; 2 mg/mL CaCl ₂ | 45.3 ± 0.4 |

composition, organic solvent in the oily phase, W2 composition and volume ratio of W1/O. The release behaviors of PLGA microspheres i.e., MS, MS-H and MS-C with different BSA encapsulation style were also studied in the present study. The detailed conditions for the preparation of PLGA microspheres in this study are listed in Tables 1 and 2.

Variation of the Internal Structure of PLGA Microspheres

A schematic representation of the proposed sequence for preparation events was depicted in Fig. 1. PLGA microspheres were successfully prepared using modified double-emulsion method. It was postulated that the PLGA microspheres were formed through three processes. First, the inner aqueous phase W1 was dispersed in the oily O phase to create the primary emulsion. Then, the primary emulsion was dispersed in a large volume of aqueous CaCl₂ solution to obtain the double-emulsion. Finally, water diffused from W1 into W2 via both osmotic pressure and diffusion mechanisms. Because there are carboxy groups in PLGA molecular, therefore some carboxy groups would exist on the surface of the droplets in the double emulsion. The Ca²⁺ has ability to bind carboxy group, therefore there may be ionic interactions generated between CaCl₂ and PLGA. Because of the Ca²⁺ ions adsorbed onto the droplets surface, the dispersive phase coalescence or phase separation during solvent evaporation may be inhibited. Removal of the solvent made the PLGA precipitated, thereby encapsulating the inner aqueous phase within a spherical polymeric matrix.

The SEM images of the obtained PLGA microspheres was shown in Fig. 2a, it displayed that microspheres were not uniform, and the size of the microspheres distributed from several hundred nanometers to the dozens of microns (Fig. 2g). To observe the internal structure of the microspheres with different size under the same preparation condition, TEM images of the different sized microspheres were shown in Fig. 1. When the diameter was smaller than 200 nm, the PLGA microspheres showed single core and multi-cores structure. The hollow microspheres were observed in the diameter range of 200–700 nm and their shell thickness was about 70 nm. The inner aqueous phase distributed randomly in the large microspheres (diameter >700 nm), and PLGA microspheres with multi-cores structure were obtained. The morphology of the double-emulsion was characterized under optical microscope (Fig. 1), and it showed that different size of droplets existed in the double emulsion and it also could be seen that several small aqueous phases dispersed in each large droplet.

The different size of the droplets brought in to the microspheres with different diameters. It was reported that in the early stage of the double-emulsion formation process, many droplets

with different diameters were created, and usually several small W1 droplets were encapsulated in one particle [27]. In the primary emulsion and double-emulsion formation processes of the modified double emulsion method, many droplets with different sizes were obtained in this study (Fig. 1). These different size of droplets underwent the solvent evaporation and polymer solidification, and converted into microspheres with different sizes, as shown in Fig. 2a. Because the W1 phases were not stable, the deformation, breakup and coalescence of the droplets would occur during the second emulsification and droplets solidification processes. It has been reported that the dispersed inner aqueous phase droplets could aggregate and spontaneously coalesce within the embryonic microspheres shortly after the second emulsification process began [28–30]. As the viscosity increased during the droplets solidification, higher viscosity of the continuous phase reinforced the viscous stress, and therefore induced droplet deformation and elongation. The collisions and simultaneous coalescences engulfed the intervening continuous phase, and then the structure involving multiple droplets within one droplet was generated [31]. In this experiment, the different degree of the W1 phase collisions and coalescences in the different size of the droplet in the double emulsion contributed to the different internal structure. And the morphology and internal structure of the PLGA microsphere would be determined by the coalescence extent of the W1 phase and the solidification rate of the polymer. In some droplets, the emulsion instability dominated the inner aqueous phase coalescence in the smaller dispersion and produced the solid and hollow core. Although for the biggest or smallest droplets, the solvent removal and polymer solidification rate were fast, no enough time provided for the W1 phases in the droplets to complete coalescence, and then the incorporation of aqueous phase in the polymer matrix resulted in the multi-core structure. The diameter range was thought to be lower than 200 nm for solid core microspheres, 200–700nm for hollow microspheres, and lower than 200 nm and greater than 700 nm for multi-core structure microspheres, as shown in Fig. 1. Base on these conclusions, the internal structure of the PLGA microspheres could be tailored by changing the process parameters to fulfill different needs.

Effect of Volume Ratio (W1/O) on the Preparation of PLGA Microspheres

The volume of inner aqueous phase was critical for primary emulsion stability, which also affected the morphology and internal structure of the PLGA microspheres. The morphology was shown in Fig. 2a–c. From the SEM images, it could be seen that smooth and spherical microspheres were prepared under different volume ratio of W1/O. The TEM results of the

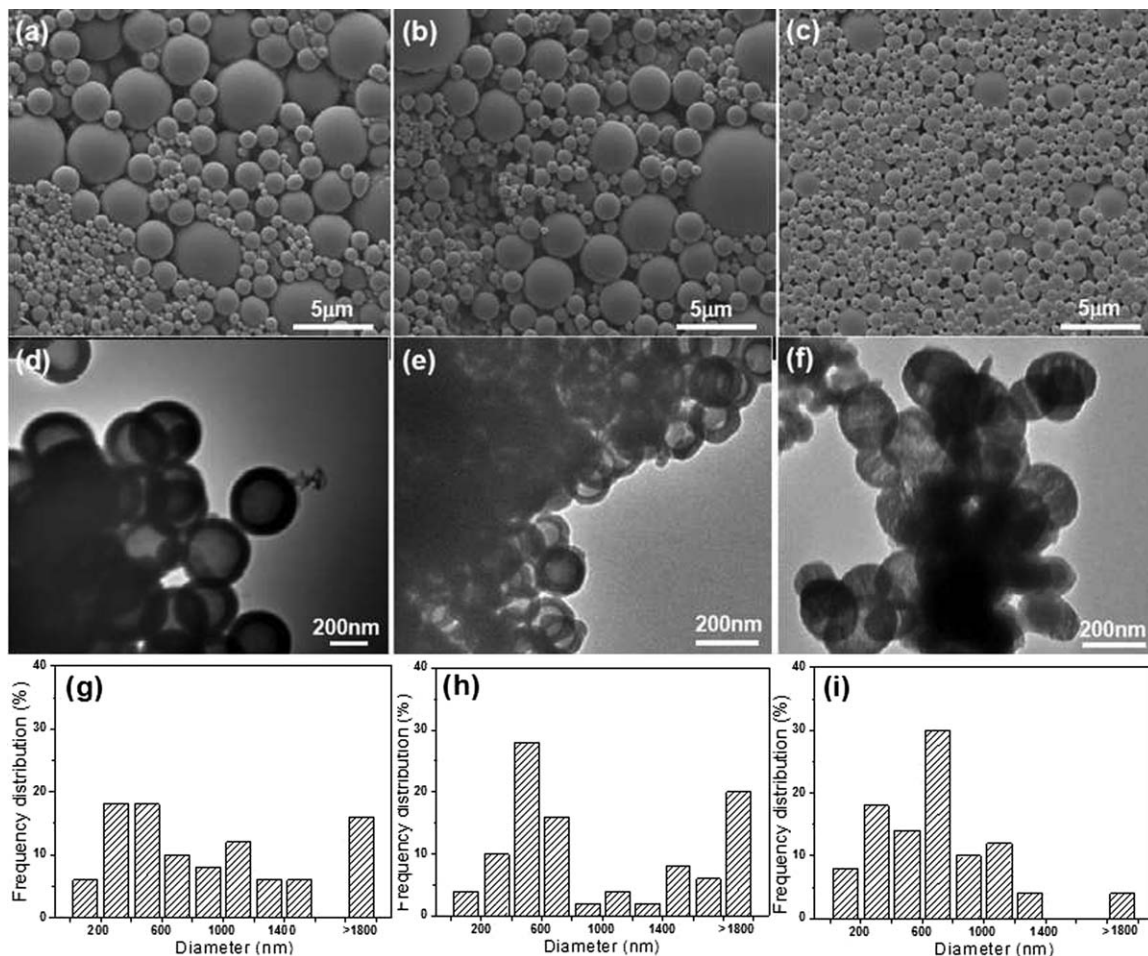


FIG. 2. SEM (a-c), TEM (d-f) micrographs and the size distributions (g-i) of PLGA microspheres prepared in different volume ratios of W1/O in the primary emulsion. (a,d) W1/O = 1/3; (b,e) W1/O = 1/5; (c,f) W1/O = 1/10. Detailed conditions are shown in Table 1 (A1–A3).

different microspheres were displayed in Fig. 2d–f. The analysis of the internal structure was presented taking the microspheres with similar size (about 200 nm) for example, and it showed that the microspheres with diameter of about 200 nm prepared from both 1/3 and 1/5 values for W1/O showed hollow structure, but when the W1/O volume ratio was set at 1/10, the PLGA microspheres exhibited multi-core structure. The size distributions of the different microspheres were demonstrated in Fig. 2g–i. The average diameters of the microspheres with 1/3, 1/5, and 1/10 of W1/O values were 875 ± 309 nm, 729 ± 179 nm, and 338 ± 32 nm, respectively. And it displayed the PLGA microspheres prepared from 1/10 showed narrower size distribution than others.

The effect of the inner aqueous phase volume on the size and morphology of microspheres had been reported and it could be confirmed that the microspheres became larger as the inner aqueous phase volume increased [32]. It was assumed that the dispersive droplets could coalesce to a single larger droplet or several multiple droplets [32]. Because of the different W1/O, the droplets generated in the double emulsion would be in different size. And this resulted in the different size distributions of the obtained microspheres, as shown in Fig. 2g–i. The droplet sizes generated were smaller when the W1/O was 1/10 than 1/3

and 1/5. Therefore, more smaller size of the W1 phases in 1/10 of W1/O value would be in the polymer droplets after second emulsification than 1/3 and 1/5. The microspheres about 200 nm in diameter formed hollow structure when the W1/O was 1/3. But when the W1/O became 1/10, the W1 phases were too small to form the hollow core because of the faster polymer solidification rate leaving no enough collision chances for the smaller dispersive inner aqueous phase coalescing. The results demonstrated that smaller and narrower size distribution microspheres could be prepared by decreasing W1/O, but the internal structure would be varied for the microspheres with approximately 200 nm in size.

Effect of the W1 Composition on the Morphology of PLGA Microspheres

The effect of the composition in the inner aqueous phase on the morphology of microspheres was investigated in this section. Figure 3a–d showed the representative SEM images of PLGA microspheres with various W1 compositions. It could be seen that the microspheres had smooth surface and almost perfect sphericity. The average diameters of the microspheres with PBS, PBS and BSA, carboxymethyl chitosan, and carboxymethyl

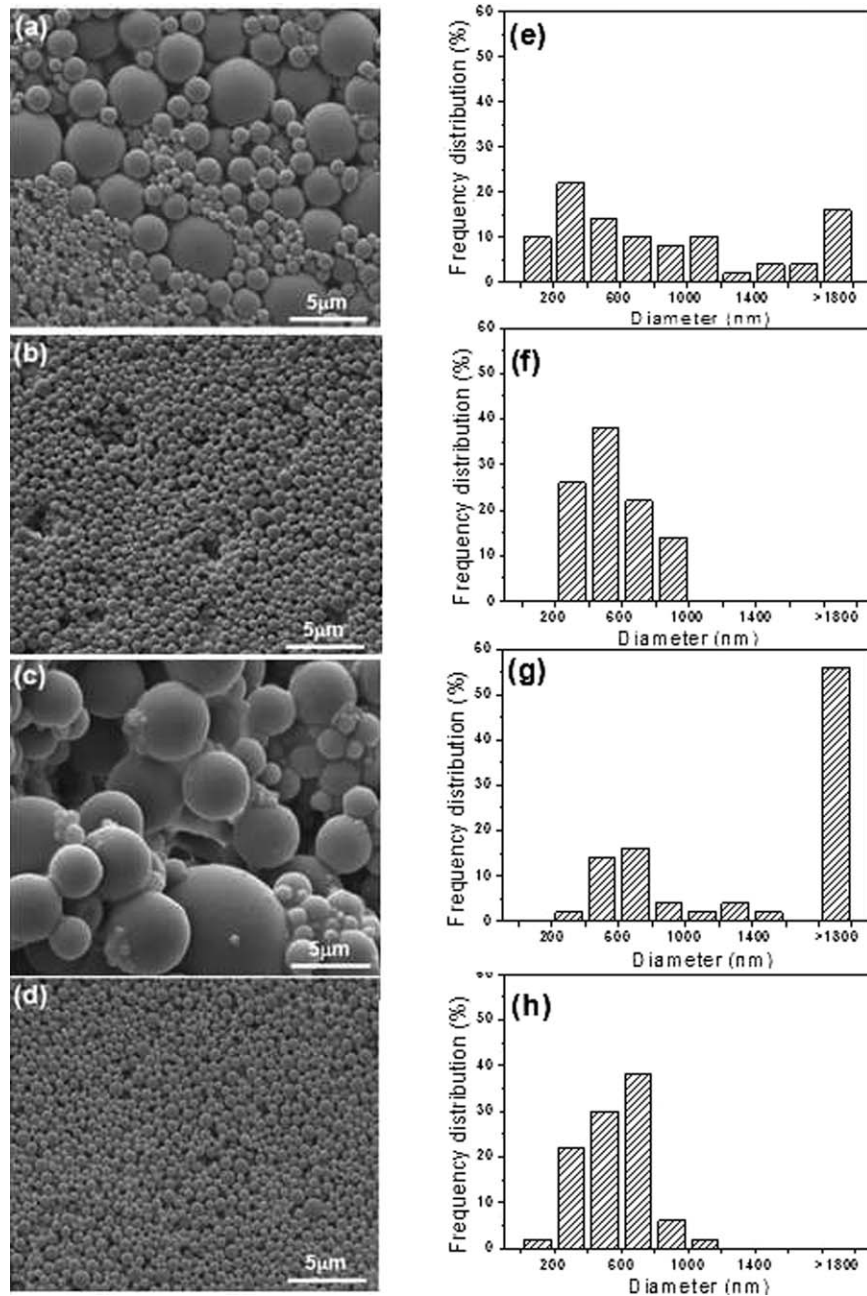


FIG. 3. SEM micrographs (a-d) and the size distributions (e-h) of PLGA microspheres prepared in different W1 solutions. (a) PBS; (b) BSA (10 mg/mL); (c) carboxymethyl chitosan (50 mg/mL); (d) BSA (10 mg/mL) and carboxymethyl chitosan (50 mg/mL). Detailed compositions are shown in Table 1 (B1–B4).

chitosan and BSA in the W1 phase were 1227 ± 1690 nm, 548 ± 190 nm, 2406 ± 1895 nm, and 552 ± 202 nm, respectively. And the size distributions of the different microspheres were demonstrated in Fig. 3e–h. Different sizes of PLGA microspheres from hundreds of nanometers to tens of micrometers were obtained under the given conditions only with PBS as W1, but the size would be narrower after introduction of BSA. Similarly, when carboxymethyl chitosan was added into W1, PLGA microspheres with relatively wide size distribution were prepared, but after addition of BSA, uniform PLGA microspheres were generated. From the size distribution results, it also could be seen that the diameter of the microspheres was in the range of 200–800 nm

after introduction of BSA in the W1 phase. These results indicated that the introduction of BSA in the W1 phase significantly improved the PLGA morphology prepared by the modified double-emulsion method in this experiment.

The stability of the primary emulsion had great effect on the later preparation for microspheres by double-emulsion method. BSA in the W1 phase not only benefited for forming small and uniform dispersive phases in primary emulsion, but also improved primary emulsion stability and inhibited droplet deformation and elongation before the second emulsification process. The microsphere size distribution became narrower because of the addition of BSA in the W1 phase. This phenomenon was

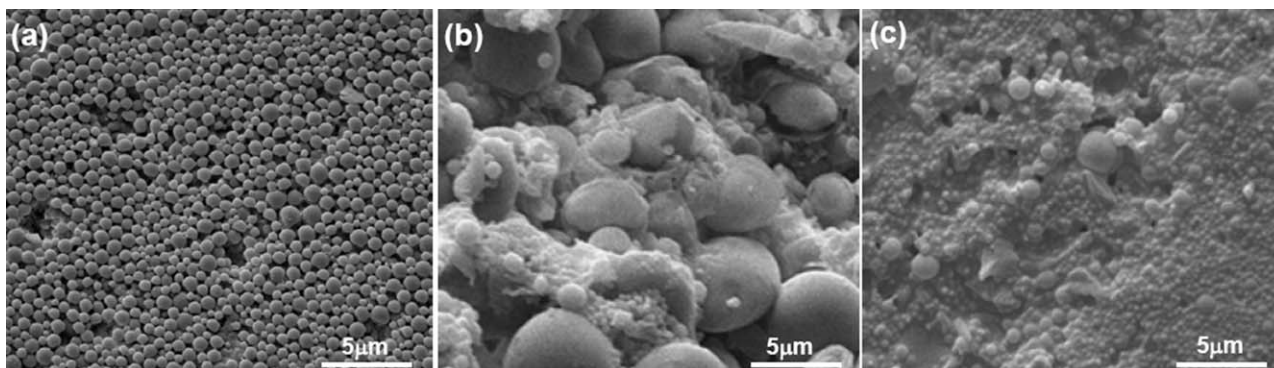


FIG. 4. SEM micrographs of PLGA microspheres prepared in different organic solvents. (a) CH_2Cl_2 ; (b) CHCl_3 ; (c) DMF. Detailed compositions are shown in Table 1 (C1–C3).

also seen for W1 contained BSA and carboxymethyl chitosan. It was reported that the high viscosity of W1 phase could hindered the W1 phase dispersing in oily phase during the emulsion formation [33]. The poor dispersion of W1 in primary emulsion was blamed for the wider size distribution, but introduction of BSA improved the dispersive property of W1 in oily phase. It was possible that BSA was a protective protein not only used for protecting some bioactive substances and growth factors, but also useful for preparing uniform microspheres by the modified double-emulsion in this experiment.

Effect of the Organic Solvent on the Morphology of PLGA Microspheres

Different organic solvents were used in the modified double-emulsion process to investigate the effects on the microspheres morphology. It was noticed that the microspheres in Fig. 4a had smaller sizes (between 200 and 700 nm) in comparison with those in Fig. 4b,c. The SEM micrographs revealed that when CH_2Cl_2 was replaced by CHCl_3 , the regular sphere-like particles showed morphological damage, and some incomplete microspheres were in sight (Fig. 4b). For the use of DMF, no integrated and smooth microsphere was obtained, and they seemed likely to be buried in the polymer matrix, but the microparticle size was significantly smaller as compared with the particles prepared in CHCl_3 (Fig. 4c).

There were two stages for the solidification of microspheres, solvent extraction and solvent evaporation, and the rate of solvent extraction and solvent evaporation were dependent on its solubility in water and boiling point, respectively [34]. The faster extraction rate could lead to faster removal of solvent from the nascent polymer droplets and quicker hardening [35]. The rapid solidification of the droplet in the double-emulsion was important, because this could reduce the dispersive droplets deforming, elongating and merging. The boiling point of CH_2Cl_2 , CHCl_3 , and DMF was 39.6, 61.2, and 153°C, respectively. With CH_2Cl_2 as the organic solvent, integrated and smooth PLGA microspheres were prepared. The microspheres with worse non-spherical morphology were obtained with CHCl_3 and DMF as organic solvents, because the solvent had slower evaporation rate and droplet deforming, elongating and merging more easily happened during CHCl_3 and DMF removal. Another reported important factor in determining the polymer

solidification process was the water solubility with the organic solvent, because the solvent diffused into aqueous phase depended on the water solubility of the organic solvent and its removal from the water/air interface by evaporation [36]. The solubility of DMF in water was better than CH_2Cl_2 and CHCl_3 , and its diffusion into the outer aqueous phase was easier which was favorable for fast solidification of dispersion droplets in the outer aqueous phase and resulted in the smaller particles. Moreover, the remained portion of DMF contributed to the bonding of the microspheres. The low boiling point and water insolubility with the organic solvent were important factors to gain integrated and smooth microspheres in this study.

Effect of the W2 Composition on the Morphology of PLGA Microspheres

Four different W2 compositions were used to evaluate the influence of W2 composition on microspheres morphology. Figure 5a–d revealed the morphology of the microspheres prepared with different W2 composition. It was obviously that several big microspheres about 20 μm were obtained (Fig. 5a). Addition of a certain amount of NaCl into W2 exhibited slight effect on the microsphere morphology, as shown in Fig. 5b. It was seen that the addition of CaCl_2 (1 mg/mL) evidently improved the morphology of the obtained microspheres (Fig. 5c). As shown in Fig. 5d, uniform and smaller microspheres were obtained using 2 mg/mL of CaCl_2 . The average diameters of the PLGA microspheres prepared with H_2O , NaCl, 1 mg/mL of CaCl_2 and 2 mg/mL of CaCl_2 as the W2 phase were 2422 ± 4055 nm, 2841 ± 4819 nm, 1370 ± 1270 nm, and 1123 ± 1221 nm, respectively. And the size distribution results in Fig. 5e–h demonstrated that the microspheres prepared using 2 mg/mL of CaCl_2 as W2 had narrowest distribution, and the diameter of most of the microspheres was in the range of 200–1200nm. The results showed that there was a strong connection between W2 composition and microspheres morphology.

The NaCl solution was used as solidification solution for double-emulsion in the previous report [34], but it showed slight effect on the microspheres in this study, and Ca^{2+} ions was thought to dominate the finally PLGA microsphere morphology as well. High concentration of CaCl_2 resulted in high osmotic

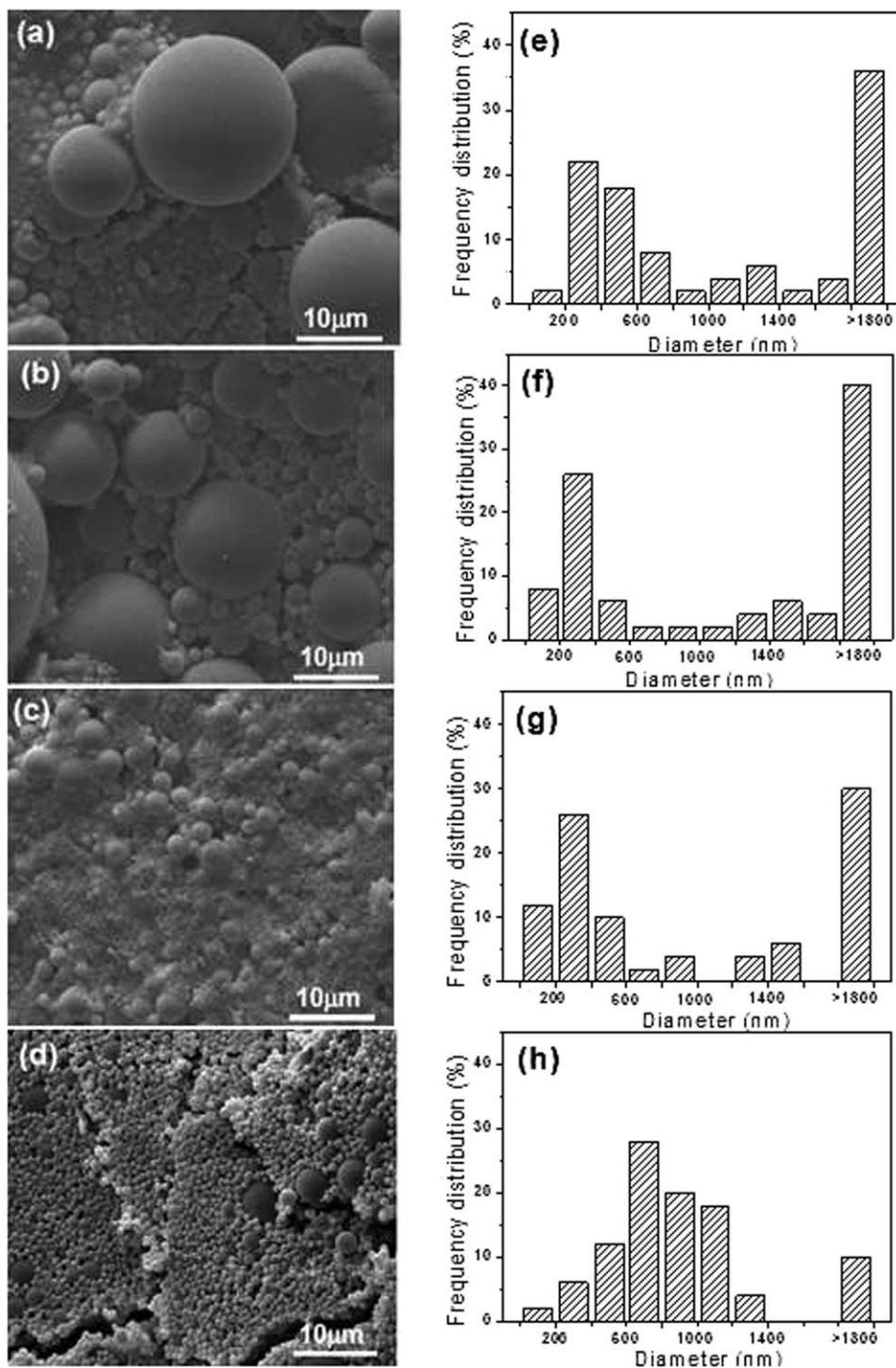


FIG. 5. SEM micrographs (a–d) and the size distributions (e–h) of PLGA microspheres prepared in different W2 solutions. (a) Deionized water; (b) 2 mg/mL NaCl; (c) 0.5 mg/mL CaCl₂; (d) 2 mg/mL CaCl₂. Detailed compositions are shown in Table 1 (D1–D4).

pressure and fast solidification of the droplet on one hand, the Ca²⁺ ions distributed on the surface of the droplet and the charge repulsion limited the coalescence of different small droplets on the other hand. The presence of Ca²⁺ resulted in better stability of the droplets in the W2 phase, which accelerated the droplets solidification and prevented droplet deformation and coalescence to obtain narrow size distribution microspheres.

In Vitro Release Behaviors of PLGA Microspheres With Different Internal Structures

The microspheres with different internal structures, which the drugs were loaded in the particle core or polymer matrix, presented a promising route for controlled drug release behavior. To evaluate the release behavior for bioactive protein, BSA was chosen as protein model and loaded into different microspheres.

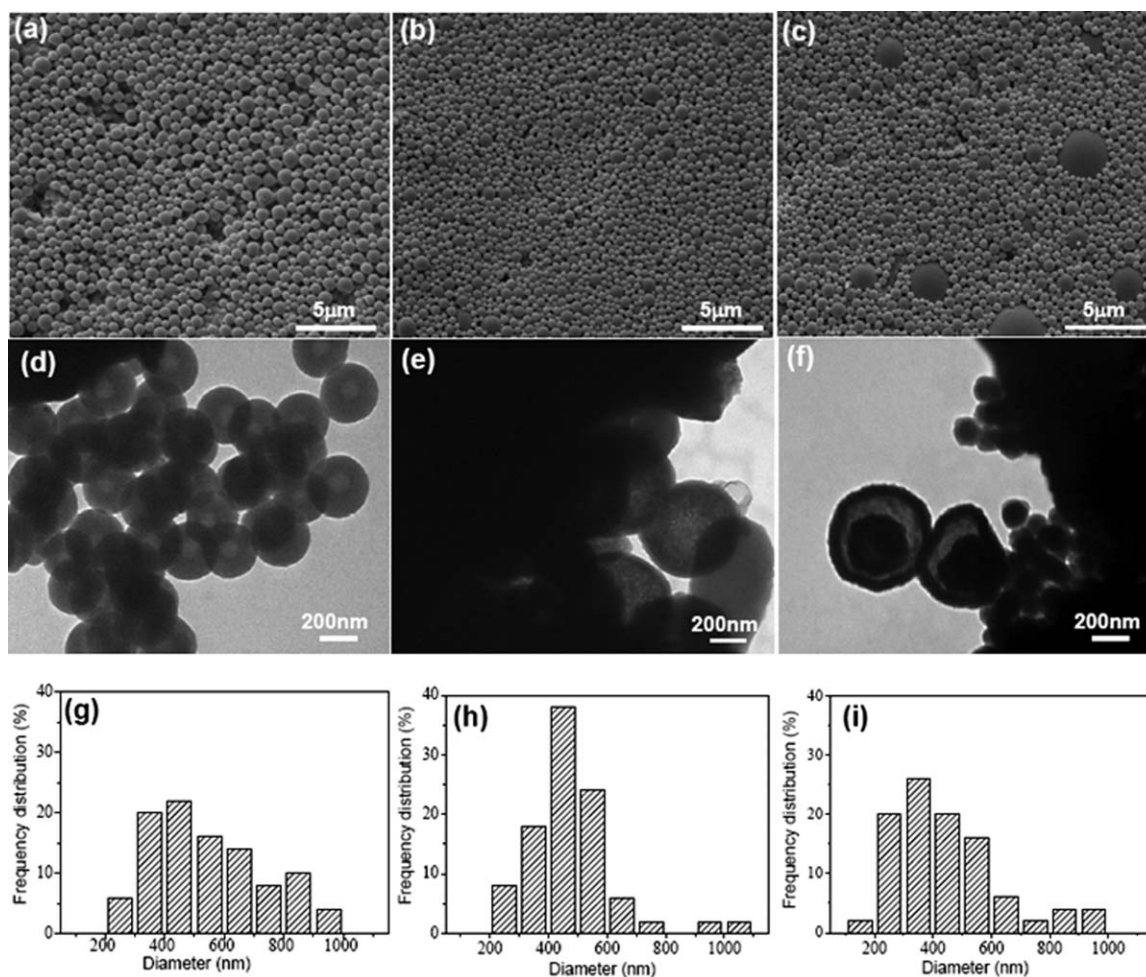


FIG. 6. SEM micrographs (a-c), TEM micrographs (d-f) and the size distributions (g-i) of PLGA microspheres for *in vitro* release of BSA. (a,d,g) MS; (b,e,h) MS-H; (c,f,i) MS-C. Detailed preparation conditions are shown in Table 2.

The preparation conditions of MS, MS-H and MS-C were shown in Table 2. Figure 6a–c displayed the SEM micrographs for the obtained microspheres. To characterize the internal structure of the microspheres, the TEM results of MS, MS-H, and MS-C were given in Fig. 6d–f. Figure 6g–i represented that the MS exhibited diameter in the range of 200–1000 nm, whereas for MS-H and MS-C, the size distribution became narrow, most distributed at 200–700 nm. It could be seen that the vacant core of the MS decreased compared with no BSA-loading microspheres, and BSA was considered to be closed to the PLGA shell, as shown in Fig. 6d. For MS-H, it showed multi-core, and the BSA was thought to be randomly distributed in the PLGA matrix (Fig. 6e). As shown in Fig. 6f, the MS-C microspheres showed solid core where BSA distributed in.

According to the spreading coefficient theory, the two materials in the different phases tended to separate during the process of solvent removal, and make themselves in the most thermodynamically stable way if enough time was given [37]. Three possible configurations including complete engulfing, partial engulfing and no engulfing could happened on the interface of the two phases [38], and various factors, such as solvent, temperature and nature of the polymers, affected the final configuration of the two polymers [39]. The PLGA in oily phase was insoluble with the

materials in internal water phase, during the fabrication process, PLGA tended to migrate towards the outer aqueous phase and precipitated to form the shell layer. At the following emulsification process, the internal water droplets coalescences were inhibited by the heparin, and dwelled in the PLGA phase to form the multi-core structure. As described before, chitosan would result in poor dispersion of W1. The large amounts of BSA also showed electrostatic interaction with carboxymethyl chitosan, and these factors produced some large W1 phases in the primary emulsion. At the initial stage of the second emulsification, one droplet may contain just one large W1 phase, after the solvent removal and polymer solidification, solid microsphere was gained. The gap between the solid core and the polymer shell generated by the phase separation and shrinkage in the droplet solidification demonstrated the above explanation.

To investigate the effects of W1 composition and the internal structure of the PLGA microspheres on the BSA release behaviors, negative heparin sodium and positive carboxymethyl chitosan were added into W1, so that BSA was encapsulated in MS, MS-C and MS-H where BSA were located in, the interface of the empty core and PLGA shell (hollow microsphere), the single core and the multi-core, respectively. The BSA encapsulation efficiencies of MS, MS-H, and MS-C were $28.7 \pm 0.4\%$,

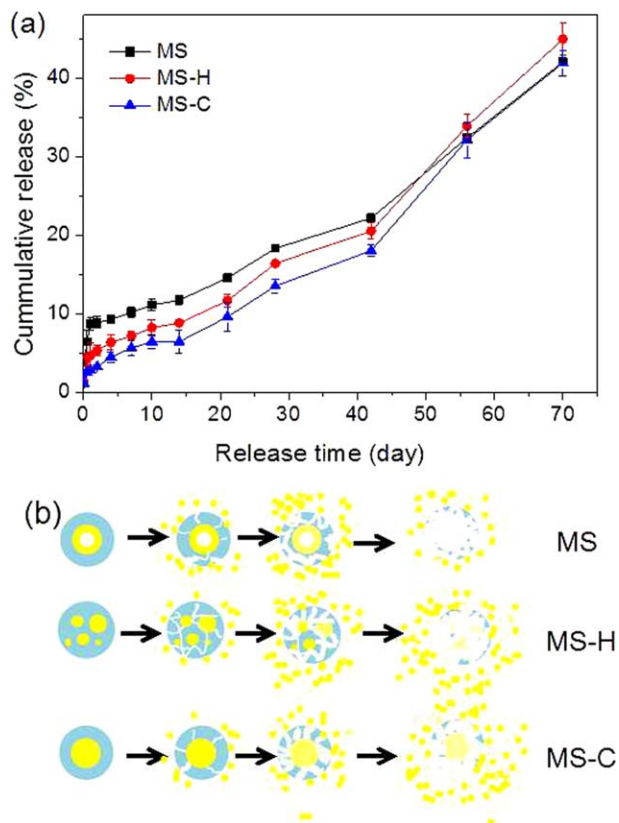


FIG. 7. *In vitro* release behaviors of BSA from MS, MS-H, MS-C microspheres (a), and the schematic representation of BSA (yellow) loading patterns, respectively (b). [Color figure can be viewed in the online issue, which is available at wileyonlinelibrary.com.]

$39.4 \pm 0.9\%$, and $45.3 \pm 0.4\%$, respectively. MS-C showed the highest encapsulation efficiency, and the encapsulation efficiency of MS-H was also higher than sample MS.

Figure 7 represented BSA loading patterns in MS, MS-H and MS-C microspheres and *in vitro* release behavior. Figure 7a showed the *in vitro* BSA release behavior for MS, MS-H and MS-C. The burst releases were all lower than 5%, and both MS-H and MS-C exhibited lower burst release. Following the initial release, a relatively faster release was observed within 2 d for MS, and the release rate slowed down between 2 and 42 d, exhibiting approximate linear relationship for all the samples. During this period, the three samples showed semblable release rates, and the MS had the highest cumulative release. However, at the last release stage (42–70 d), both the MS-H and MS-C showed faster release rate than MS sample. Figure 7b was obtained based on the TEM images in Fig. 6d–f, and the release process was proposed. The MS sample with hollow internal structure showed a faster release rate than others, because the diffusion crossed the thin shell was easier than others. The MS-H sample showed a slower release rate because the BSA distributed in the matrix randomly, and the BSA released depending on the diffusion and matrix degradation. For MS-C sample, both the polymer shell and the carboxymethyl chitosan core sustained the BSA release, then it showed slowest release rate than others. But during the final period of the release, its rate accelerated because of the relative more BSA release from the microspheres. The results indicated that addition of both the heparin and carboxymethyl chitosan could improve the encapsulation

efficiency, meanwhile decrease the burst release and prolong release periods.

From the results, it showed that the encapsulation efficiency increased after introduction of carboxymethyl chitosan and heparin in the W1 phase. A possible explanation for the higher loadings could be proposed based on the role of the W1 composition. Compared with conventional PLGA microspheres, the encapsulation efficiency of alginate-chitosan-PLGA microspheres increased, and the alginate-chitosan core could also reduce the activity loss of protein [21]. In this experiment, the addition of heparin increased W1 viscosity and protected BSA activity, and then higher encapsulation efficiency for MS-H was obtained. As a negative protein, BSA interacted with positive carboxymethyl chitosan, inhibited itself diffuse from W1 into W2. Therefore, a higher encapsulation efficiency of BSA than MS-H sample was achieved in MS-C sample. It was reported that many channels and internal pores formed by coalescence between the droplets and water phase during microsphere solidification process [1], through these channels hydrophilic drug diffused near the microspheres surface and resulted in the strong burst effect [2]. All the samples showed triphase profiles as shown in the reference [40]. The first stage of BSA release was considered as the protein loaded in the shell of MS and MS-C or the polymer matrix of MS-H. In contrast to MS-C and MS-H, more BSA loaded in the shell for MS, and it showed the fastest release rate and highest cumulative release. And, the second stage contributed to the BSA presented in the core of MS, MS-C and MS-H. After the BSA release from the shell or polymer matrix, more channels formed, and made BSA release much easily and faster. Increasing with the release time, faster rate were obtained in the third stage. Heparin was negative and a growth factor protective and sustained release substance, whereas carboxymethyl chitosan was positive which may be used to control proteins delivery. These provided the potential applications for the different kinds of the prepared microspheres.

CONCLUSIONS

By the modified double-emulsion method, PLGA microspheres with single core, multi-core and hollow internal structures were successfully prepared, respectively. A high BSA content in W1 phase and suitable ratio of W1/O, organic solvent with fast evaporate rate, and suitable concentration of Ca^{2+} ion in the outer aqueous phase benefited for uniform microspheres. And, the internal structure of the PLGA microspheres showed relevant with the size distribution. Compared with the hollow PLGA microspheres, the MS-H and MS-C microspheres showed single core and multi-core structure, and the MS-H and MS-C exhibited higher loading efficiencies and slower release rate than MS, and MS-C showed the slowest release rate. The different microspheres prepared in this experiment may be useful in loading negative charge biomolecules (DNA) and positive charge proteins (growth factors).

REFERENCES

1. M. Ye, S. Kim, and K. Park, *J. Control. Release*, **146**, 241 (2010).
2. Y. Wei, Y.X. Wang, W. Wang, S.V. Ho, F. Qi, G.H. Ma, and Z.G. Su, *Langmuir*, **28**, 13984 (2012).

3. J.M. Anderson and M.S. Shive, *Adv. Mater. Deliver. Rev.*, **212**, 64 (2012).
4. W. Wang, M.J. Zhang, R. Xie, X.J. Ju, C. Yang, C.L. Mou, D.A. Weitz, and L.Y. Chu, *Angew. Chem. Int. Ed.*, **52**, 8084 (2013).
5. Q.X. Xu, S.H. Chin, C.H. Wang, and D.W. Pac, *Biomaterials*, **34**, 3902 (2013).
6. K. Wei, X. Peng, and F. Zou, *Int. J. Pharm.*, **464**, 225 (2014).
7. H. Zhao, F. Wu, Y. Cai, Y. Chen, L. Wei, Z. Liu, and W. Yuan, *Int. J. Pharm.*, **450**, 235 (2013).
8. S. Freitas, H.P. Merkle, and B. Gander, *J. Control. Release*, **95**, 185 (2004).
9. A. Taluja and Y.H. Bae, *Mol. Pharm.*, **4**, 561 (2007).
10. G.D. Fu, G.L. Li, K.G. Neoh, and E.T. Kang, *Prog. Polym. Sci.*, **36**, 127 (2011).
11. X.W. Lou, L.A. Archer, and Z.C. Yang, *Adv. Mater.*, **20**, 3987 (2008).
12. B. Wei, S.J. Wang, H.G. Song, H.Y. Liu, J. Li, and N. Liu, *Pet. Sci.*, **6**, 306 (2009).
13. B. Albuquerque, M.S. Costa, I.N. Peça, and M.M. Cardoso, *Polym. Eng. Sci.*, **53**, 146 (2013).
14. Y. Sato, Y. Kawashima, H. Takeuchi, and H. Yamamoto, *Eur. J. Pharm. Biopharm.*, **55**, 297 (2003).
15. S.K. Sahoo, J. Panyam, S. Prabha, and V. Labhasetwar, *J. Control. Release.*, **82**, 105 (2002).
16. E. Cohen-Sela, M. Chorny, N. Koroukhov, H.D. Danenberg, and G. Golomb, *J. Control. Release.*, **133**, 90 (2009).
17. J.B. Dou, Q.Y. Zhang, M.L. Ma, and J.W. Gu, *J. Magn. Magn. Mater.*, **324**, 3078 (2012).
18. L. Wang, H. Liang, F. Wang, L.Y. Huang, Z.P. Liu, and Z.X. Dong, *Langmuir*, **29**, 5863 (2013).
19. J. Wu, T.T. Kong, K.W.K. Yeung, H.C. Shum, K.M.C. Cheung, L.Q. Wang, and M.K.T. To, *Acta Biomater.*, **9**, 7410 (2013).
20. W.J. Cui, J.Z. Bei, S.G. Wang, G. Zhi, Y.Y. Zhao, X.S. Zhou, H.W. Zhang, and Y. Xu, *Inc. J. Biomed. Mater. Res. Part B: Appl. Biomater.*, **73**, 171 (2005).
21. X.L. Zheng, Y.Z. Huang, C.H. Zheng, S.Y. Dong, and W.Q. Liang, *AAPS J.*, **12**, 519 (2010).
22. F.X. Han, X.L. Jia, D.D. Dai, X.L. Yang, J. Zhao, Y.H. Zhao, Y.B. Fan, and X.Y. Yuan, *Biomaterials*, **34**, 7302 (2013).
23. H.N. Yang, J.H. Choi, J.S. Park, S. Y. Jeon, K. D. Park, and K.H. Park, *Biomaterials*, **35**, 16 (2014).
24. F.X. Han, H. Zhang, J. Zhao, Y.H. Zhao and X.Y. Yuan, *J. Biomater. Sci., Polym. Ed.*, **24**, 1244 (2013).
25. J.R. Eisenbrey, O. Mualem Burstein, and M.A. Wheatley, *Polym. Eng. Sci.*, **48**, 1785 (2008).
26. S. Galindo-Rodriguez, E. Allémann, H. Fessi, and E. Doelker, *Pharma. Res.*, **21**, 1428 (2004).
27. K.W. Chun, H.S. Yoo, J.J. Yoon, and T.G. Park, *Biotechnol. Prog.*, **20**, 1797 (2004).
28. S. Tcholakova, N. Vankova, N.D. Denkov, and T. Danner, *J. Colloid. Interf. Sci.*, **310**, 570 (2007).
29. N. Vankova, S. Tcholakova, N.D. Denkov, I.B. Ivanov, V.D. Vulchev, and T. Danner, *J. Colloid. Interf. Sci.*, **312**, 363 (2007).
30. N. Vankova, S. Tcholakova, N.D. Denkov, V.D. Vulchev, and T. Danner, *J. Colloid. Interf. Sci.*, **313**, 612 (2007).
31. S. Kumar, *Chem. Eng. Sci.*, **51**, 831 (1996).
32. G. Crotts and T.G. Park, *J. Control. Release.*, **35**, 91 (1995).
33. H. Wu, C.Y. Liao, Q.Y. Jiao, Z. Wang, W.Z. Cheng, and Y. Wan, *React. Funct. Polym.*, **72**, 27 (2012).
34. Y. Wei, Y.X. Wang, L.Y. Wang, D.X. Hao, and G.H. Ma, *Colloid. Surface B*, **87**, 399 (2011).
35. E.J. Pollauf and D.W. Pack, *Biomaterials*, **27**, 2898 (2006).
36. S. Tiwari and P. Verma, *Int. J. Pharm. Life Sci.*, **2**, 998 (2011).
37. K.J. Pekarek, J.S. Jacob, and E. Mathiowitz, *Adv. Mater.*, **6**, 684 (1994).
38. Y.Y. Yang, M. Shi, S.H. Goh, S.M. Mochhala, S. Ng, and J. Heller, *J. Control. Release*, **88**, 201 (2003).
39. K. Leach, K. Noh, and E. Mathiowitz, *J. Microencapsul.*, **16**, 153 (1999).
40. W. Wei, L. Yuan, G. Hu, L.Y. Wang, J. Wu, X. Hu, Z.G. Su, and G.H. Ma, *Adv. Mater.*, **20**, 2292 (2008).